Suleiman *et al.*
Environmental Sciences Europe (2024) 36:131
https://doi.org/10.1186/s12302-024-00954-1

Environmental Sciences Europe

RESEARCH

Open Access

Performance of zero-valent iron immobilized on activated carbon cloth for the removal of phenol from wastewater

Muhammad Yusuf Suleiman[1], Opeoluwa Olusola Fasanya[2*], Abdulazeez Yusuf Atta[1], Fei Ye[3], Joydeep Dutta[3*] and Baba El-Yakubu Jibril[1]

Abstract

Background Discharge of large amounts of untreated industrial effluent into water bodies pose significant environmental challenges worldwide. This is due to the limitations of traditional wastewater treatment methods in the treatment of recalcitrant organic pollutants. Fenton processes involves the generation of hydroxyl radicals that are well suited to degrade organics in effluent water. This study focuses on reducing slag generation during Fenton processes and enhancing the reuse of nano-zero-valent iron (NZVI) through the immobilization of NZVI on activated carbon cloth (ACC) through a chitosan (CH) linker with phenol as a model pollutant.

Results Microstructural and spectroscopic techniques were employed to study the materials prepared and 37.5 wt% iron loading was achieved. Phenol degradation of 96.3% at 40 °C at pH of 3.0 with 50 mM H_2O_2 was achieved using ACC-CH-NZVI. Adsorption and degradation studies carried out using ACC-CH-NZVI catalyst revealed that phenol adsorption onto ACC-CH-NZVI fits the Langmuir isotherm model, following the pseudo-second-order kinetic model and first-order reaction kinetics. Thermodynamic studies indicate the non-spontaneous, endothermic and irreversible nature of the removal process. Comparing ACC-CH-NZVI with ACC and ACC-CH, phenol removal using ACC drops from 87.8 to 39%, while using ACC-CH, the removal efficiency drops from 73 to 20.9% and using ACC-CH-NZVI, phenol removal drops from 96.3 to about 70% and total organic carbon removal drops from 79 to about 60% with minimal iron leaching, highlighting the superior performance of ACC-CH-ZVI and the role of NZVI in enhancing phenol removal.

Conclusions The catalyst demonstrated good stability for phenol degradation to about 70% phenol removal from simulated wastewater and 60% TOC removal from industrial wastewater after five treatment cycles with minimal Fe leaching.

Keywords Phenol, Nano-zero-valent iron, Chitosan-coated activated carbon, Wastewater treatment, Fenton catalyst

*Correspondence:
Opeoluwa Olusola Fasanya
ope.fasanya@narict.gov.ng
Joydeep Dutta
joydeep@kth.se
Full list of author information is available at the end of the article

Graphical abstract

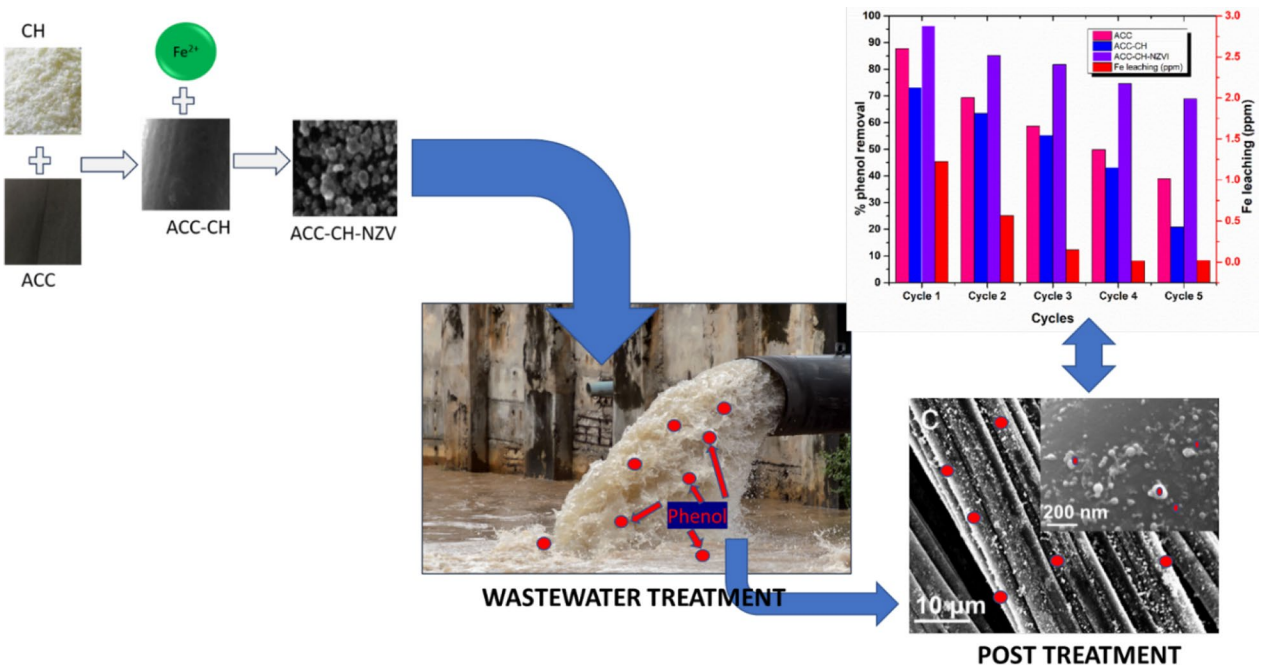

Background

Considering the discharge of substantial volumes of industrial effluents into water bodies and the environment, the relentless issue of water and environmental pollution in general has become a matter of paramount concern. Petroleum refineries typically produce a significant volume of wastewater. This is due to large amounts of water used in a variety of refining operations such as cooling systems, crude desalting, distillation, hydrotreating as well as maintenance and shutdown [1]. Processing a barrel of crude oil typically requires an average of 300 L of water leading to formation of large volumes of wastewater which contains phenols, oils, phosphates, nitrates and other highly persistent pollutants [2].

Phenol and phenolic compounds are recalcitrant organic materials found in the effluents of petroleum refineries. They are also found in the waste streams of phenolic resin manufacturing, petrochemicals and fine chemicals manufacturing industries [3]. The refractory and biotoxicity of phenol necessitates specific treatment to remove or reduce their concentration to levels necessary to allow for direct discharge into the surrounding water bodies [4].

There are various technologies available for the treatment of industrial effluents. They include traditional treatment technologies such as coagulation, flocculation, membrane separation, activated carbon adsorption, and biological approaches including nature-based solutions [5]. These treatment techniques cannot, however, eradicate the recalcitrant compounds and involve the transfer of non-biodegradable waste into sludge, giving rise to secondary pollution. Therefore, further treatment is essential for safe disposal [6]. Application of advanced oxidation processes (AOPs) such as the Fenton process, ultrasonic irradiation and microwave, using heterogeneous catalysis serve as a potential alternative technology for the destruction of this non-biodegradable portion of the waste [7]. These processes involve in situ generation of highly reactive species, such as hydroxyl radical, hydrogen peroxide, ozone and sulfate radical, characterized by low selectivity of attack. Oxidation potential of hydroxyl radicals $^{\bullet}OH$ ($E^{\circ} = 2.8$ V|SHE) and sulfate radicals ($SO_4^{\bullet -}$) ($E^{\circ} = 2.44$ V|SHE) are adequate to oxidize most of the organic contaminants. Among the advanced oxidation processes (AOPs), the Fenton process has been observed to exhibit high reactivity and efficient remediation of contaminants due to its high efficiency, feasible control, low cost and eco-friendly nature [8].

A major parameter that influences the performance of heterogeneous Fenton processes is the choice of the iron-based material. Due to the size-dependent properties, high reactivity and large specific surface area of

nanomaterials, they have found applications extensively in groundwater and soil remediation, and wastewater treatment [9]. Nano-zero-valent iron has attracted the attention of numerous scientists in wastewater treatment due to its greater degradation efficiency, low toxicity, and cost-effectiveness that are due to the nanoparticle size leading to higher surface area that render high reactivity ultimately assisting fast reaction kinetics [10]. Nanoparticles, however, tend to aggregate in solutions during treatment due to the changes in surface charge leading to direct mutual attraction between nano-particles via van der Waals forces or chemical bonds further requiring the wastewater filtration to remove the iron sludge formed during neutralization. In order to remedy this limitation, immobilizing NZVI on catalyst supports such as alumina, bentonite, kaolin, zeolite, and activated carbon has been explored [11]. Activated carbon has large number of mesopores and micropores that aid in enhanced physisorption, and due to its excellent chemical and hydrothermal stability, it is an ideal catalyst support [12].

Lütke et al. [13] demonstrated that activated carbon derived from black wattle bark waste exhibited a remarkable removal efficiency of 96% for phenolic compounds in a simulated industrial effluent. Agarwal et al [14] investigated the co-adsorptive removal of phenol and cyanide using chitosan and achieved removal percentages of 61% and 91%, respectively, at a 30 g/L adsorbent dose. It was noted that the use of activated carbon powder for adsorption might lead to secondary pollution, and modifications can potentially enhance phenol removal. Yehia et al. [15] utilized the ultrasound-assisted advanced Fenton process and achieved 75% phenol removal after 60 min using nano-zero-valent iron (NZVI) particles with hydrogen peroxide. However, issues such as NZVI aggregation and leaching were observed. Dong et al. [16] further investigated the enhancing effects of activated carbon-supported NZVI on anaerobic digestion of phenol-containing organic wastewater, achieving an 81% removal of phenol, while Messele et al. [17] reported greater than 90% conversion of phenol using nanoscale zero-valent iron supported on activated carbon powders, with satisfactory stability and some reuse of the catalyst.

Raji et al. [8] employed chitosan-coated activated carbon cloth-supported NZVI (ACC-CH-NZVI) as a Fenton catalyst for the degradation of melanoidin in wastewater achieving significant color (84.7%) and chemical oxygen demand (COD) reduction (76%) with minimal (< 2%) iron leaching after five treatment cycles. The chitosan linkers contributed to fixing the iron particles on the carbon surfaces reducing particle removal from the catalyst supports and could increase the potential of the Fenton catalyst for the removal of other recalcitrant compounds in industrial effluents. Furthermore, there is still a gap in understanding the optimal conditions and mechanisms of adsorption for using NZVI supported on activated carbon as a Fenton catalyst for efficient phenol removal. Therefore, this research aims to fill this gap by investigating the application of NZVI supported on activated carbon cloth coated with chitosan as a Fenton catalyst for the removal of phenol in wastewater, with a focus on understanding the removal efficiency, mechanism of sorption of the catalyst and the reusability potential using both a simulated phenol-containing wastewater and an industrial wastewater.

Materials and methods

Materials

Activated carbon cloth (ACC) was purchased from Chemviron Carbon Ltd., Houghton-le-Spring, UK. Chitosan (from crab shells) was obtained from Sigma-Aldrich. Analytical grade sodium hydroxide (NaOH), iron (II) sulfate heptahydrate ($FeSO_4$ $7H_2O$), sodium borohydride ($NaBH_4$), hydrogen peroxide (H_2O_2, 30 wt%), 1-ethyl-3-(3-dimethylaminopropyl) carbodiimide (EDC), and N-hydroxysuccinimide (NHS) were purchased from Sigma-Aldrich Chemie GmbH, Taufkirchen, Munich, Germany. Phenol (C_6H_5OH, crystals) was purchased from Molychem, Mumbai, India. Glacial acetic acid was purchased from BDH Laboratory Supplies Poole, England. Nitric acid (69%) was purchased from VWR International GmbH, Langenfeld, Germany. Hydrochloric acid (37%) was purchased from Loba Chemie while sodium acetate buffer (pH 4.7) was prepared and used for all experiments.

Synthesis of chitosan-coated activated carbon cloth impregnated with NZVI

Chitosan-coated activated carbon cloth was synthesized by the chemical cross-linking method [8]. The double woven activated carbon cloth (500 mg) was first immersed in 40 ml of 1 mM EDC solution for 5 min, followed by adding 10 ml of 1 mM NHS solution and shaking for another 5 min. It was then rinsed with deionized water and placed in 2% chitosan solution for 1.5 h under shaking. The chemically crosslinked chitosan-coated activated carbon was rinsed with deionized water and kept for drying in the ambient overnight.

The prepared chitosan-coated activated carbon was dipped in aqueous solutions of 0.2 M $FeSO_4$ for 3 h under nitrogen bubbling for the chelation of Fe^{2+} ions with chitosan. To flush out excess ions, it was diluted using a mixture of ethanol and deionized water (v/v 1:1) five times the volume of the mixture. 100 mL of 0.2 M $NaBH_4$ was then added dropwise into the slurry at 25 °C with magnetic stirring and N_2 bubbling for 30 min to reduce Fe^{2+} to NZVI. The synthesized activated carbon impregnated

with NZVI was separated from the mixture and subjected to further Fe^{2+} chelation and reduction process to increase the amount of NZVI loading. It was then washed with acetone three times before vacuum drying at 60 °C.

Characterization of the catalyst

The structural morphology and the elemental composition of the synthesized catalysts was analyzed on a scanning electron microscope (SEM–EDX, GEMINI Ultra 55, Oberkochen, Germany). The chemical interaction within chemically crosslinked chitosan-coated activated carbon cloth catalyst and that with NZVI impregnation was examined by Fourier transform infrared spectroscopy (FT-IR Spectrometer Nicolet iS10, Thermo Fisher Scientific, Waltham, USA).

Catalyst activity in the treatment of phenol-containing wastewater

A stock solution of 1000 mg/L phenol was prepared with distilled water and stored in a refrigerator until required. Working solutions of 200 mg/L were prepared by diluting the stock solution with distilled water just before use.

The catalyst's performance was evaluated by the degradation of 10 ml of 200 mg/L phenol-containing wastewater stirred constantly at 200 rpm in a 50 ml beaker through a Fenton reaction. A H_2O_2 concentration of 30 mM (the stoichiometric concentration required to mineralize 200 mg/L phenol) was used initially for the experiment. The pH of the solution was adjusted to 3.0, 4.0, 5.0 and 6.0 using 0.1 M HCl or 0.1 M NaOH as required, and the reaction temperature was set initially to 30 °C. A reaction time of 90 min was used throughout the experiment. For each treatment cycle, the treated solution was tested for phenol removal using a UV–Vis spectrophotometer by recording the changes in optical absorbance at 275 nm [18]. The pH value that gave the highest percentage of phenol removal was used in subsequent treatments. H_2O_2 concentration of 30, 50 and 70 mM was then varied, and the optimal concentration was used in subsequent steps. The reaction temperature was also varied to determine the best temperature for the degradation process. The removal efficiency was tested at 30, 35, and 40 °C. The optimum reaction temperature was recorded and used for subsequent analysis.

The activity of the other two adsorbents, activated carbon and chitosan-coated activated carbon, were studied as control experiments at optimum conditions for one cycle and compared to the activity achieved using chitosan-coated activated carbon with NZVI impregnation.

Catalyst reusability

Based on optimum conditions obtained, the chitosan-coated activated carbon impregnated with NZVI was studied for reusability to treat phenol-containing wastewater. After the first cycle treatment, the catalyst was removed from the treated solution, washed with deionized water, and used for another treatment cycle using a freshly prepared phenol solution. The cycle was repeated five times using the same catalyst. After each treatment cycle, a sample from the solution was tested for phenol removal and iron leaching was recorded using a microplasma atomic emission spectrophotometer (MP-AES Agilent 4200).

The efficiency of the catalyst was also tested on refinery wastewater for iron leaching and total organic carbon content (TOC) using the Walkley–Black method by oxidizing the organic carbon with chromate in the presence of sulfuric acid and titrating with ammonium ferrous sulfate solution [19].

Results and discussion

Characterization of activated carbon-supported NZVI

The functional groups present on ACC-CH and ACC-CH-NZVI were observed using the FT-IR and the spectra are presented in Fig. 1. A broad peak between 3700 and 3000 cm^{-1} was observed in all three catalysts, with the peak centered at 3350 cm^{-1} from O–H stretching vibrations of the carboxylic groups present on activated carbon [20]. At 3400 cm^{-1}, N–H stretching vibrations overlapped with the O–H band in ACC-CH and ACC-CH-NZVI due to the presence of an amino group from chitosan, which resulted in broader peaks for the ACC-CH and ACC-CH-NZI catalysts [21]. The presence of bands at 2931 cm^{-1} for ACC-CH and 2910 cm^{-1} for ACC-CH-NZVI are due to C–H stretching vibrations of chitosan. There is a shift in the C–H vibration frequency for ACC-CH-NZVI due to the addition of NZVI. Peaks at 2952 cm^{-1} for AC-CH and 2907 cm^{-1} for AC-CH-NZVI are due to the C–H stretching vibration of the chitosan backbone due to the addition of chitosan on activated carbon [8]. C=O stretching vibrations of primary amide around 1650 cm^{-1} result from chitosan in ACC-CH and ACC-CH-NZVI. Around 1550 cm^{-1}, a less intense peak for ACC-CH-NZVI was observed for N–H bending vibrations of the amino group than that present in ACC-CH. In addition, at 1080 cm^{-1} and 1033 cm^{-1}, N–H deformative vibrations of amide were observed for ACC-CH and ACC-CH-NZVI. This overlaps with the C–O stretching vibrations at 1045 cm^{-1}, 1077 cm^{-1} and 1047 cm^{-1} in ACC, ACC-CH and ACC-CH-NZVI, respectively. Finally, as seen from the figure, a weaker band was observed at 1149 cm^{-1} for ACC-CH-NZVI due to the C–N stretching vibration of amino groups than that observed for ACC-CH at 1142 cm^{-1}. Overall, the results from FT-IR spectra demonstrate the successful

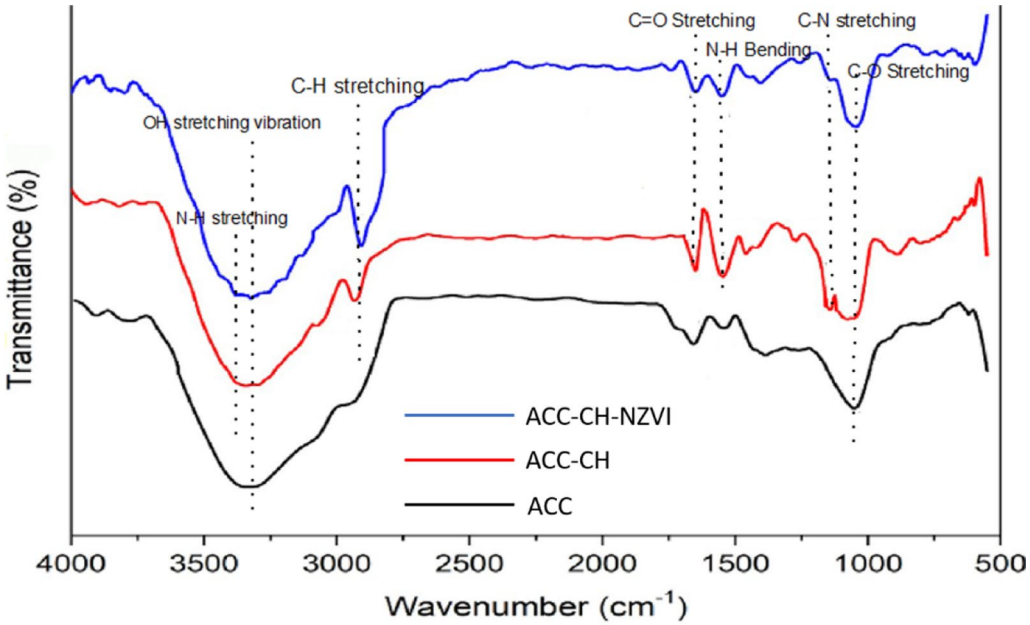

Fig. 1 FT-IR spectra for ACC, ACC-CH and ACC-CH-NZVI catalysts

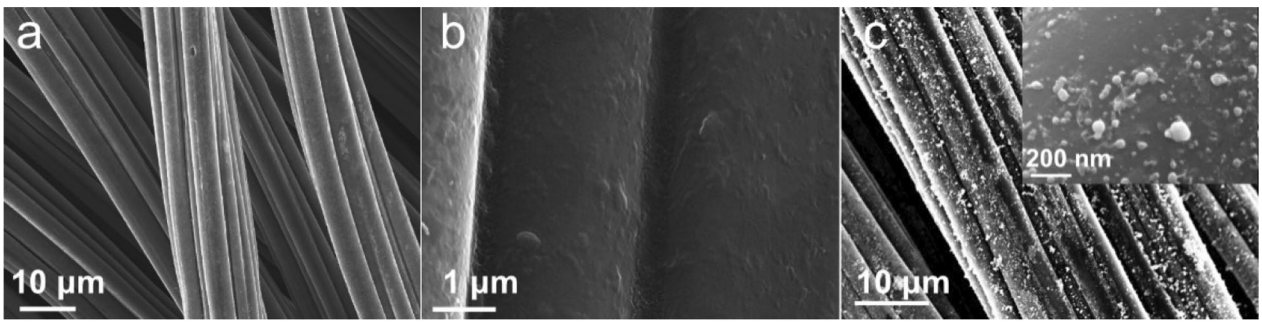

Fig. 2 SEM micrograph of **a** AC, **b** AC-CH and **c** AC-CH-NZVI

chelation of NZVI onto chitosan-coated activated carbon support.

Figure 2 shows the morphologies on surface of ACC supported catalysts. The SEM image of AC-CH indicates that after the coating of chitosan, the ACC surface was completely covered with chitosan layers. The clean and smooth surface of AC-CH can be observed. In addition to the C–H and C–N band absorption peaks from FT-IR, the presence of NZVI particles on AC-CH can also be visualized from the SEM image. The distortions on the smooth surface of AC-CH indicate that NZVI particles were dispersed and chelated on the AC-CH support. NZVI particles of sizes between 5 and 50 nm can be observed from the SEM image.

To further confirm the presence of iron nano-particles on the support as observed from the FT-IR and SEM results (energy-dispersive X-ray spectroscopy), EDX analysis was carried out for ACC-CH-NZVI to check the presence of iron particles on the catalyst surface. Table 1 shows the elemental compositions of the ACC-CH-NZVI catalyst. The carbon and oxygen presence in the catalyst is from the activated carbon cloth support and chitosan. The EDX result showed that

Table 1 Elemental composition of ACC-CH-NZVI

Element	Weight %
Carbon	36.68
Oxygen	24.35
Sodium	0.50
Aluminum	1.02
Iron	37.45

37.5 wt% iron has been immobilized on the ACC-CH support.

Catalyst activity on phenol-containing wastewater

Effect of pH on phenol degradation using ACC-CH-NZVI Fenton catalyst

Figure 3 shows the effect of different pH values on Fenton degradation of 200 mg/L phenol at 30 mM H_2O_2 concentration and 30 °C using ACC-CH-NZVI catalyst. From the Figure, the phenol degradation rate was found to decrease with increasing pH of the solution. At a pH 3.0, more H^+ are available in the solution to oxidize NZVI to Fe^{2+} (Eq. 1) which further oxidizes to Fe^{3+} for the reaction with H_2O_2 that generates the $^{\bullet}OH$ radicals which degrade phenol:

$$RX + Fe^0 + H^+ \leftrightarrow RH + Fe^{2+} + X^- \quad (1)$$

Thus, the surface of NZVI is prone to a higher degree of oxidation at acidic pH than at higher pH values [22]. As the pH increases to 6.0, a decrease in the rate of degradation was observed mainly due to a reduction in the amount of H^+, which limits the production of Fe^{2+}, leading to the lower number of •OH radicals available for phenol degradation. The decomposition of hydrogen peroxide into H_2O and O_2 and the formation of insoluble precipitates of amorphous iron hydroxides on NZVI due to higher pH could also inhibit the regeneration of Fe^{2+} and thus produce a very low number of the oxidants from reaction with H_2O_2 as reported in an earlier work [23]. At pH values lower than 3.0, excess H^+ will lead to the scavenging of •OH radicals, inhibiting their production. Excessive leaching of iron also occurs at very acidic pH, and this will affect the reusability of the catalyst (Chen et al., 2009). A pH value of 3.0 is thus considered the best condition for all subsequent experiments in this work.

Effect of H_2O_2 concentration on degradation of phenol using Fenton catalyst

The effect of hydrogen peroxide concentration as a source of hydroxyl radicals for phenol degradation is shown in Fig. 4. At 50 mM concentration, about 94% phenol degradation was achieved. Beyond 50 mM, the rate of phenol degradation begins to fall. This can be attributed to the scavenging of excess •OH radicals generating hydroperoxyl radical ($\bullet OH_2$), which can further decompose to superoxide and oxygen. This scavenging effect can be prevented by maintaining a high contaminant concentration to H_2O_2 ratio [41]. Using the stoichiometric concentration of H_2O_2, about 84% degradation was achieved, 10% lower than that achieved at 50 mM. This may be due to a smaller number of hydroxyl radicals formed.

Effect of temperature on Fenton degradation of phenol

In Fenton reactions, higher temperatures lead to faster reaction rates due to increased kinetic energy of the reactant molecules, leading to more frequent and energetic collisions, which can accelerate the formation of hydroxyl radicals with the subsequent degradation of phenol. At higher temperatures, hydrogen peroxide (H_2O_2) decomposes more rapidly, which can lead to the formation of more hydroxyl radicals [24]. From Fig. 5, within the tested temperature range, increasing the reaction temperature from 303 to 313 K, the rate of phenol degradation rises from 93.8 to 96.3% due to an increase in the formation of hydroxyl radicals from the decomposition

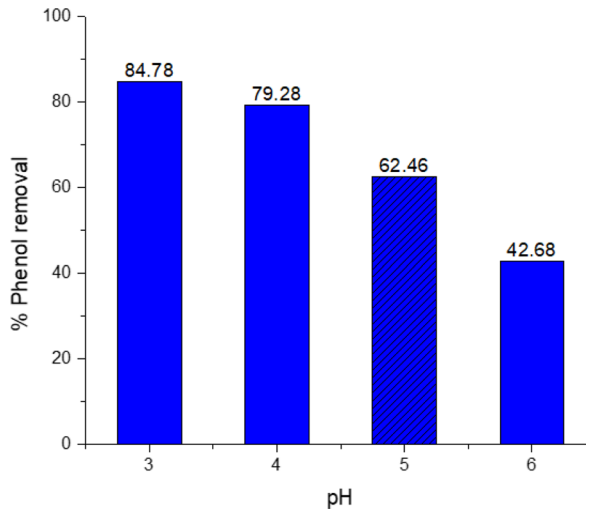

Fig. 3 Removal rate as a function of varying pH during Fenton degradation of 200 mg/L phenol using ACC-CH-NZVI ([H_2O_2] = 50 mM, temp = 30 °C)

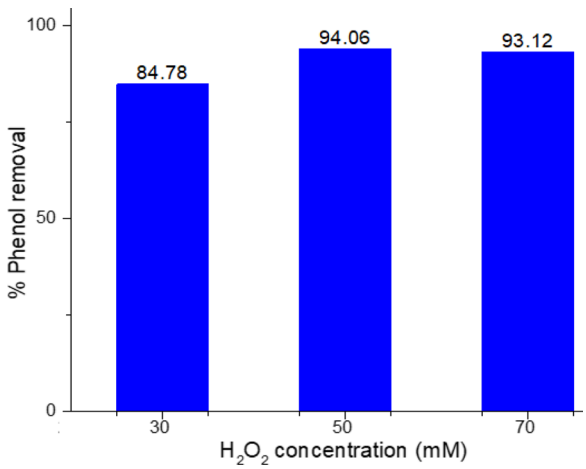

Fig. 4 Effect of H_2O_2 concentration on Fenton degradation of 200 mg/L phenol using ACC-CH-NZVI (pH = 3.0, temp = 30 °C)

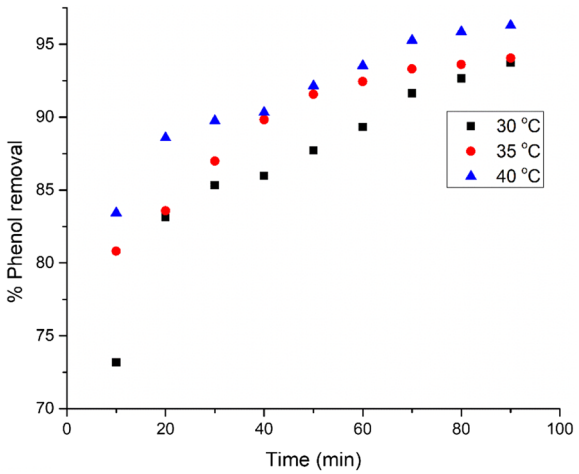

Fig. 5 Effect of reaction temperature on Fenton degradation of 200 mg/L phenol using ACC-CH-NZVI (pH = 3.0, $[H_2O_2]$ = 50 mM)

Table 2 Adsorption of phenol on ACC-CH-NZVI

Catalyst dosage (g)	Concentration C_e (mg/L)	% Removal	Adsorbate uptake q_e (mg/g)
0.05	76.1	62.0	24.8
0.1	26.1	87.0	17.4
0.15	12.5	93.8	12.5
0.2	8.0	96.0	9.6
0.25	5.6	97.2	7.8
0.3	4.1	97.9	6.5

of hydrogen peroxide at higher temperatures. However, excessive decomposition of H_2O_2 at much higher temperatures can potentially reduce their availability for the degradation of phenol due to the formation of scavengers [25], but this hypothesis was not supported by our current data.

Adsorption isotherms

Adsorption isotherms were studied for Langmuir, Freundlich, Temkin and Dubinin–Radushkevich models, to investigate the mechanism and the interaction that takes place between the adsorbate and the catalyst adsorbent (ACC-CH-NZVI). It was carried out using 200 mg/L constant phenol concentration by varying the catalyst dosage from 0.05 to 0.3 g (Table 2) at room temperature and a specific solution pH of 3.0, as the optimized pH for Fenton degradation of phenol, as mentioned earlier. Observing from Table 2, increasing the amount of catalyst to 0.3 g enhances the removal of phenol up to about 98%.

The linear form of the listed isotherms is shown in Fig. A.1 in supplementary file, and the parameters of the models are listed in Table 3. Based on the values of R^2 obtained from the plots, the Langmuir isotherm model has R^2 value of 0.9974, Freundlich isotherm model has an R^2 value of 0.9838, Temkin isotherm has an R^2 value of 0.9958 and Dubinin–Radushkevich isotherm model with R^2 value of 0.9937. All four models show a good fit with the experimental data, with the Langmuir isotherm displaying the best fit with an R^2 value of 0.9974, and was reported to be more suitable for phenol adsorption using ACC-CH-NZVI catalyst. This means that a single layer of phenol is formed homogeneously on the adsorbent surface. It also indicates that the ACC-CH-NZVI catalyst has a finite number of uniform interfacial adsorption sites for interaction with phenol [26]. This was in tandem with results reported by Xie et al. [27] on the adsorption of phenol by activated carbon. The maximum adsorption capacity, as calculated by Langmuir isotherm, was 29.94 mg/g in agreement with the work of Hernández-barreto et al. [28] on phenol adsorption using two different types of activated carbon. Langmuir isotherm constant was calculated as 0.06 L/mg, and the separation factor as 0.077 indicating favorable adsorption of phenol molecules at the specified conditions [29].

Table 3 Adsorption isotherm constants

	Qm (mg/g)	K_L (L/mg)	R_L	R^2
Langmuir	29.94	0.06	0.077	0.9974
	1/n	**K_f (mg/g)**		**R^2**
Freundlich	0.4614	3.6125		0.9838
	b (J/mol)	**K_T (L/g)**		**R^2**
Temkin	389	0.608		0.9958
	β (mol^2/kJ^2)	**E (kJ/mol)**		**R^2**
D-R	4.00E-09	11.2		0.9937

Adsorption kinetics

Three adsorption kinetic models, namely pseudo-first-order, pseudo-second-order and intra-particle kinetic models, were employed to describe the efficiency and mechanism of phenol adsorption on ACC-CH-NZVI catalyst at 313 K. From Table 4 and Fig. A.2 in supplementary file, it can be noticed that the pseudo-second-order model has the highest correlation coefficient of 0.9979, which yields the best fit out of the three models. This implies that chemisorption controls the rate of phenol adsorption on ACC-CH-NZVI, and the active surface sites on the adsorbent influence the adsorption capacity of the adsorbent. Similar observation was reported by other researchers which show that phenol adsorption onto activated carbon follows the pseudo-second-order kinetic model [26]. The pseudo-second-order adsorption kinetic rate constant, as shown in Table 4, is calculated to be 0.0587 g/gm min, and the predicted equilibrium adsorbate uptake of 11.07 mg/g.

Reaction kinetics

Two kinetic models: first-order (for reactions in which the reaction rate linearly depends on the reactant concentration) and second-order (for reactions in which the reaction rate is described as being proportional to the product of the concentrations of two reactants) kinetic models were employed to study the reaction order of phenol degradation using the ACC-CH-NZVI Fenton catalyst at different temperatures. From the plot of -ln (C_t/C_o) versus t, the first-order rate constant increases from 0.0138 min^{-1} at 303 K to 0.0172 min^{-1} at 313 K. Similarly, from the plot of $1/C_t$ versus t for second-order kinetics, the second-order rate constant increases from 0.0006 to 0.0013 L mg^{-1} min^{-1}. This increase in the value of the rate constants with an increase in temperature, as shown in Table 5, is a result of the increased kinetic energy of the reacting particles, which facilitates more collisions between the reacting molecules, leading to increased generation of hydroxyl radicals consequently increasing the reaction rate for phenol degradation [30].

From the plots in Fig. A.3 based on R^2 values, it can be observed that the first-order kinetic model fits better with the experimental data with an activation energy value of 17.375 kJ/mol. Similar results were reported by Refs. [31, 32]. However, at 308 K, second order gives the best fit with R^2 value of 0.991.

Adsorption thermodynamics

Adsorption thermodynamic parameters such as enthalpy, entropy and Gibb's free energy were studied for phenol adsorption and degradation using ACC-CH-NZVI Fenton catalyst. The influence of degradation temperature between 303 and 313 K was investigated in order to determine the nature of the process. An increase in phenol degradation was observed with an increase in the adsorption temperature. This may be due to good

Table 4 Adsorption kinetic model constants

Pseudo-first order	**k (min^{-1})**	**Qe (mg/g)**	**R^2**
$\ln(q_e - q_t) = lnq_e - K_1 t$	0.0464	6.75	0.9079
Pseudo-first order	**k (g/mg min)**	**Qe (mg/g)**	**R^2**
$\frac{t}{q_t} = \frac{1}{K_2 q_e^2} + \frac{t}{q_e}$	0.0587	11.07	0.9979
Intra-particle model	**k_p (mg $min^{1/2}$/g)**		**R^2**
$q_t = K_p t^{\frac{1}{2}} + C$	1.24		0.843

Table 5 Reaction kinetic constants for phenol degradation using ACC-CH-NZVI

First-order kinetics	**T (K)**	**k_1 (min)**	**E_A (kJ/mol)**	**R^2**
$-\ln\left(\frac{Ct}{Co}\right) = kt$	303	0.0138	17.375	0.9766
	308	0.0156		0.9524
	313	0.0172		0.9651
Second-order kinetics	**T (K)**	**k_2 (L/mg min)**	**E_A (kJ/mol)**	**R^2**
$\frac{1}{C_t} = \frac{1}{C_o} - kt$	303	0.0006	60.876	0.9303
	308	0.0008		0.991
	313	0.0013		0.9125

reaction interactions between the adsorbate and the functional sites on the catalyst [33]. Adsorption enthalpy (ΔH) and entropy (ΔS) were calculated using Erying equation (Eq. 2). ΔH was calculated from the slope of the graph of ln (k/T) versus 1/T, while ΔS from the intercept as seen in Fig A4 in supplementary file. The Gibb's free energy value (ΔG) was calculated using Eq. 3 to check the spontaneity of the process:

$$\ln(k/T) = \ln(k_b/h) + \Delta S/T - \Delta H/RT \quad (2)$$

where k is the first-order rate constants obtained from kinetic study, k_b is the Boltzmann constant and h is the Planck's constant.

$$\Delta G = \Delta H - T\Delta S \quad (3)$$

The free Gibbs energy (ΔG) for adsorption of phenol increased from 64.2 to 65.8 kJ/mol with increase in temperature from 303 to 313 K, demonstrating that the adsorption process is non-spontaneous and that some energy is needed to drive the adsorption process [26]. These data are presented in the supplementary file in Table A1.

The positive value obtained for the adsorption enthalpy (14.2 kJ/mol) due to the adsorbent–adsorbate interactions with contributions possibly from Van der Waals forces (4–10 kJ mol^{-1}), hydrophobic bond forces (about 5 kJ mol^{-1}), hydrogen bond forces (2–40 kJ mol^{-1}) and dipole bond forces (2–29 kJ mol^{-1}) indicated the endothermic nature of the reactive adsorption process.

The negative entropy change ΔS obtained as − 162.8 J/mol K indicates the lower structural freedom of the transition state formed compared to the reactants, low irregularities in the adsorption of phenol by ACC-CH-NZVI, and irreversibility of the degradation process [34].

Catalyst reusability

It is important to assess the stability and reusability of the ACC-CH-NZVI catalyst for use in practical engineering applications. Phenol forms a weak acidic solution existing in the molecular form that has a large affinity to activated carbon. To evaluate the role of ZVI in contaminants degradation, the phenol removal process was tested with the other two prepared catalysts by reusing the catalysts for five cycles of treatment. After each cycle, the adsorbent was removed from the treated solution and washed with distilled water. As observed from Fig. 6a, ACC-CH-NZVI displays greater efficiency (96.29%) in phenol removal than ACC (87.71%) and ACC-CH (73.09%). The good phenol removal efficiency by ACC is due to its preeminent characteristics for adsorption [35]. The decrease in phenol removal from 89.86% by ACC to 71.01% by ACC-CH is due to blockage of some surface-active sites when chitosan is coated on activated carbon cloth. The mechanism by which phenol is adsorbed onto ACC involves the formation of complexes between the activated carbon surface and the aromatic ring of phenol, π–π interaction between phenolic ring and activated carbon basal planes, and hydrogen bonding between the phenol molecules [36].

As observed from Fig. 6a for all the three catalysts, phenol removal efficiency decreases with an increase in the number of treatment cycles for all the three adsorbents.

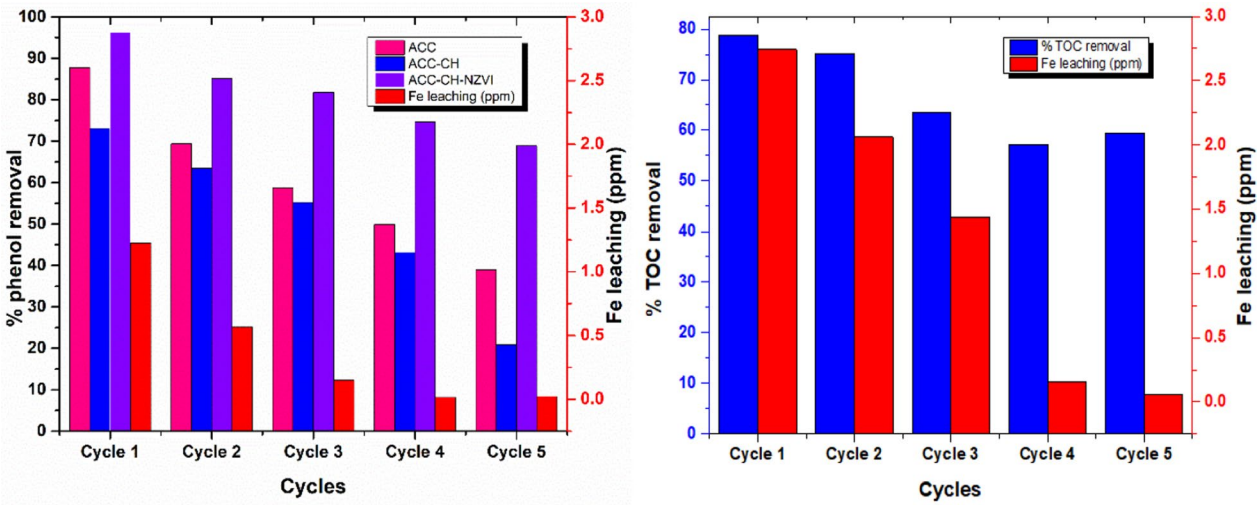

Fig. 6 Reusability of catalyst using **a** 200 mg/L phenol-containing wastewater for ACC, ACC-CH and ACC-CH-NZVI, **b** industrial wastewater for ACC-CH-NZVI

Using ACC-CH-NZVI, phenol degradation efficiency decreases from 96.3 to 68.9% after five cycles, while using ACC, 87.7% phenol removal was recorded after the first cycle and drops to 39% after the fifth cycle. For ACC-CH, the removal efficiency drops from 73.1 to 20.9%. This highlighted that phenol molecules adsorbed do not cross-contaminate ACC-CH-NZVI catalyst and that NZVI plays a role in the Fenton degradation of phenol. The mechanism by which Fenton reactions degrade phenol involves ferrous ions (Fe^{2+}) reacting with hydrogen peroxide (H_2O_2) to produce ferric ions (Fe^{3+}), hydroxide ions (OH^-), and hydroxyl radicals ($^{\bullet}OH$) (Eq. 4). The hydroxyl radicals attack the phenol molecule, initiating the oxidation process leading to the formation of hydroxylated intermediates (hydroquinone and catechol) (5). Further oxidation of these intermediates by hydroxyl radicals involves the abstraction of hydrogen atoms, leading to the formation of benzoquinone (Eq. 6). On further attack, the aromatic ring is cleaved resulting in the formation of carboxylic acids (Eq. 7–9) which can be easily mineralized (10–11). At the molecular level, the phenol molecules interact with the chitosan-coated NZVI via hydrogen bonding and electrostatic interactions facilitated by the functional groups in chitosan (e.g., $-NH_2$ and $-OH$ groups). These interactions can enhance the adsorption of phenol onto the catalyst surface, promoting more efficient degradation [37, 38]:

$$Fe^{2+} + H_2O_2 \rightarrow Fe^{3+} + OH^- + \cdot OH \quad (4)$$

$$C_6H_5OH + 2 \cdot OH \rightarrow C_6H_4(OH)_2 + H_2O \quad (5)$$

$$C_6H_4(OH)_2 + 2 \cdot OH \rightarrow C_6H_4O_2 + 2H_2O \quad (6)$$

$$C_6H_4O_2 + 4 \cdot OH \rightarrow C_4H_4O_4 + C_2H_4O_2 \quad (7)$$

$$C_4H_4O_4 + 4 \cdot OH \rightarrow 2C_2H_2O_3 + 2H_2O \quad (8)$$

$$C_2H_2O_3 + 2 \cdot OH \rightarrow C_2H_2O_4 + H_2O \quad (9)$$

$$C_2H_2O_4 + 2 \cdot OH \rightarrow 2CO_2 + 2H_2O \quad (10)$$

$$C_2H_4O_2 + 6 \cdot OH + 2CO_2 + 4H_2O \quad (11)$$

ACC-CH-NZVI was also used to treat industrial wastewater using the optimum conditions achieved for phenol degradation. 78.86% of total organic carbon content removal was recorded after the first treatment cycle for the industrial wastewater. This decreases to about 60% (Fig. 6b) after the fifth treatment cycle. This decrease in treatment efficiency for both the simulated and industrial wastewater may be related to the loss of active sites on the catalyst surface due to deactivation, aggregation of NZVI on the support, precipitation of iron species or poisoning of the surface of the catalyst from products of Fenton reaction [39].

In order to confirm whether the leaching of iron from ACC-CH-NZVI into the two wastes has occurred, after each treatment cycle, the treated water was tested for iron concentration using microwave plasma atomic emission spectrometry (MP-AES). The results from MP-AES show minimal iron leaching. As shown in Fig. 6b, after the first treatment cycle, 1.226 ppm of iron was detected in the simulated solution and 2.743 ppm of iron in the industrial waste. The higher concentration of iron in the treated water for industrial waste may be due to the complex nature of the waste containing various phenolic compounds that can accelerate iron leaching. In addition, for both wastes, corrosion of the NZVI surface by passivation may lead to high leaching of iron in the first treatment cycle [40]. The leaching was reasonably stable in the fourth cycle. Fe leaching into the wastewater at the fifth treatment cycle is 0.022 ppm for simulated wastewater and 0.055 for industrial wastewater, which is very low compared to the World Health Organization (WHO) permissible limit of 5 ppm. The minimal iron leaching from NZVI is due to the chelating effect of chitosan, which can adsorb the ferrous and ferric ions from the Fenton reaction, making the continuous supply of Fe^{2+} possible for better phenol degradation [8].

Conclusions

In this study, nano-zero-valent iron was immobilized on activated carbon cloth support coated with chitosan and applied in the treatment of phenol-containing wastewater. Characterization methods such as SEM, FT-IR and EDX confirmed the successful incorporation of NZVI onto the support, with substantial iron loading (38 wt%). Optimal operational conditions were found to be pH of 3.0, hydrogen peroxide (H_2O_2) concentration of 50 mM, and reaction temperature of 40 °C, resulting in phenol removal rates of 96%. Adsorption and degradation studies carried out using ACC-CH-NZVI catalyst revealed that phenol adsorption onto ACC-CH-NZVI fits the Langmuir isotherm model with $R^2 = 0.9974$, $K_L = 0.06$ L/mg and $Q_m = 29.94$ mg/g. The process follows the pseudo-second-order adsorption kinetics with $R^2 = 0.9979$ and pseudo-second-order rate constant, $k_2 = 0.0587$ g/mg min, and first-order reaction kinetics with first-order rate constant, $k_1 = 0.0172$ min^{-1} at 40 °C. Based on the thermodynamic studies carried out, the thermodynamics parameters for Gibb's free energy change, ΔG values increase from 64.2 kJ/mol at 303 K to 65.8 kJ/mol at 313 K, adsorption enthalpy, ΔH calculated as 14.8 kJ/mol and adsorption entropy, ΔS as −162.9 J/mol K indicating

that the adsorption process is non-spontaneous, endothermic, lower structural freedom, low irregularities and irreversible. The catalyst demonstrates good stability for phenol degradation to about 70% phenol removal from simulated wastewater and 60% TOC removal from industrial wastewater after five treatment cycles with minimal Fe leaching, demonstrating the good reusability of the catalyst. In comparison with ACC and ACC-CH, the superior performance of ACC-CH-ZVI and the role of NZVI in enhancing phenol degradation was highlighted. These findings hold significant promise for addressing environmental challenges posed by recalcitrant industrial pollutants like phenol. The ACC-CH-ZVI catalyst offers an environmentally friendly and cost-effective solution for removing persistent contaminants from wastewater. By exploring the outputs, this research contributes to the broader goal of sustainable industrial wastewater treatment. For accurate determination of phenol removal, we recommended the use of HPLC–UV to monitor the concentration of phenol. Further research should focus on evaluating the cost–benefit analysis of temperature increase for enhancing phenol degradation and improving the efficiency of Fenton reaction at near neutral pH.

Abbreviations

AOP	Advanced oxidation processes
ACC	Activated carbon cloth
CH	Chitosan
COD	Chemical oxygen demand
EDC	1-Ethyl-3-(3-dimethylaminopropyl) carbodiimide
EDX	Energy-dispersive X-ray spectroscopy
FT-IR	Fourier transform infrared spectroscopy
NZVI	Nano-zero-valent iron
SEM	Scanning electron microscopy
TOC	Total organic carbon

Supplementary Information

The online version contains supplementary material available at https://doi.org/10.1186/s12302-024-00954-1.

Supplementary material 1.

Acknowledgements
JD and FY would like to acknowledge support from INSPIRE project funded by the European Union under agreement ID 101112879.

Author contributions
OO Fasanya, AY Atta, J Dutta and BJ El-Yakubu conceptualized and designed the study. MY Suleiman, OO Fasanya, F Ye and AY Atta performed experimental investigation and synthesis. MY Suleiman, OO Fasanya and AY Atta carried out formal analysis and interpretation of results. The first draft of the manuscript was written by MY Suleiman. OO Fasanya, AY Atta, F Ye, J Dutta and BJ El-Yakubu reviewed and finalized draft of manuscript. F Ye, J Dutta, and AY Atta provided resources. AY Atta and J Dutta supervised the overall study. All the authors reviewed the results and approved the final version of the manuscript.

Funding
Open access funding provided by Royal Institute of Technology. F. Ye and J. Dutta received funding for some part of this work from the European Union under the Horizon Europe Programme, Grant Agreement No. 101112879 (INSPIRE).

Availability of data and materials
All data are contained within the manuscript and supplementary materials.

Declarations

Consent for publication
Not applicable.

Competing interests
The authors declare no competing interests or any competing interests.

Author details
[1]Department of Chemical Engineering, Ahmadu Bello University, Zaria, Nigeria. [2]Industrial and Environmental Pollution Department, National Research Institute for Chemical Technology, Zaria, Nigeria. [3]Functional and Nanomaterials, Department of Applied Physics, KTH Royal Institute of Technology, Hannes Alfvéns Väg 12, 114 19 Stockholm, Sweden.

Received: 6 April 2024 Accepted: 30 June 2024
Published online: 15 July 2024

References

1. Jafarinejad S, Jiang SC (2019) Current technologies and future directions for treating petroleum refineries and petrochemical plants (PRPP) wastewaters. J Environ Chem Eng 7:103326
2. Abdulredha M, Khalil AH, Ali SA, Idowu I, Amoako-Attah J (2021) Elimination of phenol from refineries effluents using electrocoagulation method. IOP Conf Ser Earth Environ Sci 877:012053
3. Jibril BY, Atta AY, Al-Waheibi YM, Al-Waheibi TK (2013) Effect of copper loadings on product selectivities in microwave- enhanced degradation of phenol on alumina-supported copper oxides. J Ind Eng Chem 19:1800–1804
4. Messele SA, Bengoa C, Stüber F, Fortuny A, Fabregat A, Font J et al (2015) Catalytic wet peroxide oxidation of phenol using nanoscale zero-valent iron supported on activated carbon. Desalin Water Treat. https://doi.org/10.1080/19443994.2014.1002011
5. Nachiyar CV, Rakshi AD, Sandhya S, Jebasta NBD, Nellore J (2023) Developments in treatment technologies of dye-containing effluent: a review. Case Stud Chem Environ Eng 7:100339
6. Singh RP, Singh PK, Gupta R, Singh RL (2019) Treatment and recycling of wastewater from textile industry. In: Singh RL, Singh RP (eds) Advances in biological treatment of industrial waste water and their recycling for a sustainable future. Springer Singapore, Singapore, pp 225–266
7. Atta AY, Jibril BY, Al-Waheibi TK, Al-Waheibi YM (2012) Microwave-enhanced catalytic degradation of 2-nitrophenol on alumina-supported copper oxides. Catal Commun 26:112–116
8. Raji M, Ahmad S, Ye F, Dutta J (2021) Nano zero-valent iron on activated carbon cloth support as Fenton-like catalyst for ef fi cient color and COD removal from melanoidin wastewater. Chemosphere 263:127945
9. Hamd WS, Dutta J (2020) Chapter 11 - Heterogeneous photo-Fenton reaction and its enhancement upon addition of chelating agents. In: Bonelli B, Freyria FS, Rossetti I, Sethi R (eds) Nanomaterials for the detection and removal of wastewater pollutants. Elsevier, Amsterdam, pp 303–330
10. Gebre SH (2023) Nanoscale zero-valent iron for remediation of toxicants and wastewater treatment. Environ Technol Rev 12:390–419
11. Chen X, Ji D, Wang X, Zang L (2017) Review on nano zerovalent Iron (nZVI): from modification to environmental applications. IOP Conf Ser Earth Environ Sci 51:012004
12. Raji M, Nazeri M, Ye F, Dutta J (2022) Prediction of heterogeneous Fenton process in treatment of melanoidin-containing wastewater using data-based models. J Environ Manage 307:114518
13. Lütke SF, Igansi AV, Pegoraro L, Dotto GL, Pinto LAA, Cadaval TRS (2019) Preparation of activated carbon from black wattle bark waste and its application for phenol adsorption. J Environ Chem Eng 7:103396
14. Agarwal B, Sengupta P, Balomajumder C (2014). Equilibrium, kinetic andthermodynamic studies of simultaneous co-adsorptive removal of

phenol andcyanide using chitosan. Int J Chem Eng. 2014;7(11): 863-870.https://doi.org/10.5281/zenodo.1336580
15. Yehia FZ, Eshaq G, Rabie AM, Mady AH, Elmetwally AE (2015) Phenol degradation by advanced Fenton process in combination with ultrasonic irradiation. Egypt J Pet 24:13–18
16. Dong D, Wang R, Geng P, Li C, Zhao Z (2019) Enhancing effects of activated carbon supported nano zero-valent iron on anaerobic digestion of phenol-containing organic wastewater. J Environ Manage 244:1–12
17. Messele SA, Bengoa C, Stüber F, Fortuny A, Fabregat A, Font J (2016) Catalytic wet peroxide oxidation of phenol using nanoscale zero-valent iron supported on activated carbon. Desalin Water Treat 57:5155–5164
18. Tetteh S, Zugle R, Adotey JPK, Quashie A (2018) Electronic spectra of ortho -substituted phenols: an experimental and DFT study. J Spectrosc 2018:1–10
19. Poudel S (2020) Organic Matter determination (Walkley-Black method). TUDelft. 2–6
20. Tajuddin Sikder M, Tanaka S, Saito T, Kurasaki M (2014) Application of zerovalent iron impregnated chitosan-caboxymethyl-β-cyclodextrin composite beads as arsenic sorbent. J Environ Chem Eng 2:370–376
21. Bahari HS, Ye F, Carrillo EAT, Leliopoulos C, Savaloni H, Dutta J (2020) Chitosan nanocomposite coatings with enhanced corrosion inhibition effects for copper. Int J Biol Macromol 162:1566–1577
22. Zhang N, Chen J, Fang Z, Tsang EP (2019) Ceria accelerated nanoscale zerovalent iron assisted heterogenous Fenton oxidation of tetracycline. Chem Eng J 369:588–599
23. Yehia FZ, Helal MH, Ali O, Elfadly AM, Mady AH, Roshdy AA (2013) Catalytic degradation of phenol using different chelating agent at near neutral pH in modified-fenton process. Egypt J Chem 56:199–212
24. Farias J, Albizzati ED, Alfano OM (2009) Kinetic study of the photo-Fenton degradation of formic acid. Combined effects of temperature and iron concentration. Catal Today 144:117–123
25. Vasquez-Medrano R, Prato-Garcia D, Vedrenne M (2018) Chapter 4 - Ferrioxalate-mediated processes. In: Ameta SC, Ameta R (eds) Advanced oxidation processes for waste water treatment. Academic Press, Cambridge, pp 89–113
26. Ma Y, Gao N, Chu W, Li C (2013) Removal of phenol by powdered activated carbon adsorption. Front Environ Sci Eng 7:158–165
27. Xie B, Qin J, Wang S, Li X, Sun H, Chen W (2020) Adsorption of phenol on commercial activated carbons: modelling and interpretation. Int J Environ Res Public Health 17:1–13
28. Hernández-barreto DF, Giraldo L, Moreno-piraján JC (2020) Dataset on adsorption of phenol onto activated carbons: equilibrium, kinetics and mechanism of adsorption. Data Br 32:106312
29. Ray SS, Gusain R, Kumar N (2020) Chapter five - Adsorption equilibrium isotherms, kinetics and thermodynamics. In: Ray SS, Gusain R, Kumar N (eds) Carbon nanomaterial-based adsorbents for water purification. Elsevier, Amsterdam, pp 101–118
30. Zazo JA, Pliego G, Blasco S, Casas JA, Rodriguez JJ (2011) Intensification of the Fenton process by increasing the temperature. Ind Eng Chem Res 50:866–870
31. Li J-z, Hu W, Wang Y, Zhong J-b, Li S-x (2012) A kinetic study of phenol oxidation with H_2O_2 catalysed by crowned Schiff base Mn(III) complexes in micellar media. Prog React Kinet Mech 37:30–41
32. Abou-Gamra ZM (2014) Kinetic and thermodynamic study for Fenton-like oxidation of amaranth red dye. Adv Chem Eng Sci 4:285–291
33. Mojoudi N, Mirghaffari N, Soleimani M, Shariatmadari H, Belver C, Bedia J (2019) Phenol adsorption on high microporous activated carbons prepared from oily sludge: equilibrium, kinetic and thermodynamic studies. Sci Rep 9:1–12
34. Ahile UJ, Wuana RA, Itodo AU, Sha R, Dantas RF (2020) Stability of iron chelates during photo-Fenton process: the role of pH, hydroxyl radical attack and temperature. J Water Process Eng 36:101320
35. Gayathiri M, Pulingam T, Lee KT, Sudesh K (2022) Activated carbon from biomass waste precursors: Factors affecting production and adsorption mechanism. Chemosphere 294:133764
36. Allahkarami E, Monfared AD, Silva LFO (2023) Toward a mechanistic understanding of adsorption behavior of phenol onto a novel activated carbon composite. Sci Rep. https://doi.org/10.1038/s41598-023-27507-5
37. Jain M, Mudhoo A, Ramasamy DL, Najafi M, Usman M, Zhu R et al (2020) Adsorption, degradation, and mineralization of emerging pollutants (pharmaceuticals and agrochemicals) by nanostructures: a comprehensive review. Environ Sci Pollut Res Int 27:34862–34905
38. Zhu L, Wang L, Xu Y (2017) Chitosan and surfactant co-modified montmorillonite: a multifunctional adsorbent for contaminant removal. Appl Clay Sci 146:35–42
39. Barzegar G, Jorfi S, Zarezade V, Khatebasreh M, Mehdipour F, Ghanbari F (2018) 4-Chlorophenol degradation using ultrasound/peroxymonosulfate/nanoscale zero valent iron: reusability, identification of degradation intermediates and potential application for real wastewater. Chemosphere 201:370–379
40. Ho M, Lee J, Young J (2019) Oxidation resistance of nanoscale zero-valent iron supported on exhausted coffee grounds. Chemosphere 234:179–186
41. Kumar SM (2011) Degradation and mineralization, of organic contaminants by Fenton and photo-Fentonprocesses: review of mechanisms and effects of organic and inorganic additives. Res J Chem Environ 15(2):96–112

Publisher's Note